Single- and Multigrain Nanojunctions with a Self-Assembled Monolayer of Conjugated Molecules

N. B. Zhitenev, A. Erbe, and Z. Bao
Bell Labs, Lucent Technologies, Murray Hill, New Jersey 07974, USA
(Received 23 September 2003; published 7 May 2004)

Systematic conductivity measurements in nanoscale junctions containing a self-assembled monolayer of conjugated molecules are reported. Different conductivity mechanisms are identified depending on the granularity of the metal used as a substrate for assembling the monolayer. Unexpectedly, the energy scale controlling the dominant conductance channels is quite low in comparison with the molecular level spacing. In single-grain junctions, the dominant conductance mechanism is hopping with an energy scale of the order of 10–100 meV determined by the nature of the metal contacts. In the case of multigrain junctions, additional tunnel conductance is observed with low-energy Coulomb-blockade features.

DOI: 10.1103/PhysRevLett.92.186805 PACS numbers: 73.63.–b, 73.23.–b, 73.40.Gk

Recently, a variety of advanced techniques have been employed to contact single or a few molecules. Some interesting effects have been reported: the negative differential conductance [1], the Kondo effects on single molecules [2,3], scaling of conductance with integral factors [4], bistable molecular devices [5].

Despite the remarkable progress, there is noticeable quantitative and qualitative discrepancy between the modeling of the transport through a single molecule and the majority of the experimental results. For typical metal-molecule contact the metal Fermi level falls in the middle of the large energy gap between highest occupied molecular orbital (HOMO) and lowest unoccupied molecular orbital (LUMO). In many experiments, however, the characteristic energy scale for the dominant transport mechanism appears to be unexpectedly small, typically of the order of 100–300 meV [6–11] instead of a few eV expected from calculations [12–14]. At the same time, conductance values measured in experiments are typically much lower than the calculated ones [12].

The vast majority of the experiments deal not with single molecules but with a small/large number of the molecules within a self-assembled monolayer (SAM). The control of the topography of the interface between the molecules and the metal is crucially important. Defects of the molecular packing occur at the grain boundaries of supporting metal [15]. The process of molecular assembly itself affects the morphology of the metal surface [16]. Metal electrodes can undesirably react with the molecules [17,18] and additional defects within SAM can be created [19] during contact fabrication.

In the present Letter we systematically study conducting properties of metal-SAM-metal junctions varying the surface topography of the metal electrodes and the size of the junctions. The dominant conductance mechanism in the junctions smaller than the size of metal grain is hopping. The characteristic energy is small (~10–100 meV) and determined by the material of the metal contacts. It suggests a common existence of low-lying energy states within monolayers usually not incorporated in theoretical models. In larger molecular junctions containing SAM assembled on multiple metal grains, the conductance does not vanish at low temperatures. The remaining tunneling conductance exists in addition to the thermally activated conductance channel.

The junctions are fabricated on sharp quartz tips [20]. The tips are the broken ends of quartz rods with square cross section drawn by a micropipette puller. First, the metal drain electrode is evaporated on one face of the sharpened rod. Next, the molecular layer is assembled on the drain electrode. The rod with SAM is placed in a vacuum evaporator and the source electrode is evaporated on the rod face opposing the drain. Then, the rod is rotated so that the sharp tip faces the evaporation target. The final evaporation of thin metal film connects the source with the drain electrode covered by the SAM. Because of the difference in the incident angle, the accumulated metal is thicker on the tip than on the slanted faces of the rod. The overall thickness is chosen so that a continuous metal film on top of the SAM is formed only in the immediate vicinity of the tip.

To vary the junction size and to investigate the role of metal topography, four different shapes of tips (Fig. 1) have been used. The tips shown in Fig. 1(a) (Sh1) and Fig. 1(b) (Sh2) are drawn using different pulling regimes. We expect that the junction area scales with the size of the tip edge. Thermally evaporated drain electrode (1 Cr/20 nm Au) exhibits grains with the size ~15–25 nm and height variation ~1.5 nm. The size of grains is comparable to the edge of tip Sh1 but smaller than the edge length ~60–80 nm of tip Sh2. Two other shapes are fabricated by plasma-enhanced chemical vapor deposition of 50 nm (Fig. 1(c), Sh3) or 100 nm (Fig. 1(d), Sh4) of SiO_2 on Sh1 tips. The motivations for these shapes are to explore properties of larger junctions and to simulate substrates rougher than the pristine

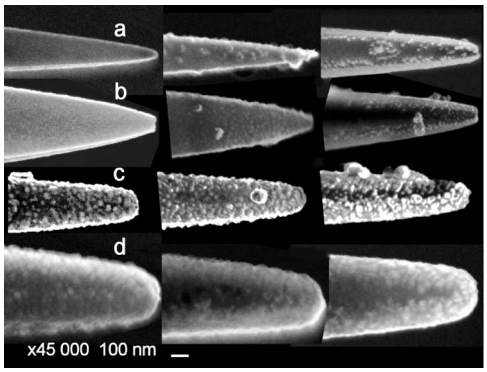

FIG. 1. Different types of junctions used in the experiment. All tips are drawn from quartz rods with a square cross section. Left column: 1 nm Cr / 20 nm Au drain electrode evaporated on top face of the tips. Center column: molecules assembled on drain electrodes. Right column: side view of the tips with both source and drain electrodes. (a) and (b) Tips are drawn using different pulling regimes. Au grain sizes ~15–25 nm, height variation ~2 nm. Grains at the edges of the films grow larger after assembly of SAM. (c),(d) Tips with ~50 and ~100 nm of SiO_2, respectively, deposited by PECVD before the metal evaporation. Grain size ~50 nm, height variation ~10 nm.

quartz that might be more typical for other types of processing [21]. The grains of the drain have a visible size ~50 nm with hight variation ~10 nm.

The molecule used in this Letter is terthiophene (T3) terminated with thiol bonding groups at both ends. This conjugated molecule forms dense monolayers [22]. Thiol terminations are commonly used links to gold [10]. The SAM is assembled on the top of the drain electrode by dipping the tip in a 50 μmol molecular solution for 5–30 min.

A few junctions are prepared simultaneously to provide better sample statistics. The conductance of two samples is monitored during the evaporation. Typically, the final metal evaporation from the tip side is stopped when conductance of the order of 10^{-7}–10^{-5} Ω^{-1} is detected on control samples. The character of conductance growth as a function of thickness varies with the type of the tip.

On Sh1 tips, measurable conductance is detected starting almost from zero thickness. It grows in a few jumps reaching a plateau as a function of thickness at 1.5–2 nm. If stopped there, the yield of good devices is high (75%). Further evaporation increases the percentage of shorted junctions. On Sh2 tips, the conductance uncontrollably jumps from undetectably small to high values typical for shorted junctions at a thickness of ~1 nm. The yield of good devices is low (10%). On both Sh3 and Sh4 tips, detectable conductance develops starting at ~1.5 nm and reaches a plateau at ~3–4 nm with the yield of good devices ~50%.

First, we discuss the results obtained for the Au-T3-Au junctions formed on Sh1 tips. A typical set of *IV* curves is shown in Fig. 2. The *IV* curves are nearly linear at room temperature over a broad range of source-drain bias (V_{sd}). The conductance significantly decreases at lower temperature.

Figure 3 shows the zero-bias conductance plotted versus inverse temperature. The dependence can be fitted sensibly with a single exponent over a significant temperature range. Such behavior is usually associated with hopping conductance. The better fit is with $\exp(-E_a/T)^{\alpha}$ with α varying from 0.6 to 0.9 for different samples. For the purpose of the present Letter the simple exponential fit is used. The determined activation energy is remarkably small: for most Au-T3-Au samples the energy is between 40 and 150 K. The activation energy distinctly depends on the type of metal electrode. The largest $E_a \sim$ 1000 K is seen for Au-T3-Pd junctions. The characteristic energies for all measured junctions with different metal electrodes are summarized in the inset to Fig. 3. Overall, the energy scale seems to be determined by the combination of both top and bottom electrodes.

Figure 4 demonstrates a typical result of measurements of the junctions made on other types of tips. In this case, the conductance of the junctions generally does not vanish as temperature is decreased. The ratio between the temperature-dependent conductance and the zero-temperature residual conductance varies significantly. We suggest that the residual conductance is a parallel conductance channel with weak temperature dependence. The temperature-dependent conductance part displays similar activated behavior. The determined activation energies are shown in the inset to Fig. 3. The data fall within the same general range as the data for the smallest junctions confirming that the temperature-dependent part of the conductance is of the same nature for all junctions.

In addition, low-temperature *IV* curves often display periodic features [20](insets to Fig. 4). The conductance peaks are spaced periodically with the same period of ~50 mV. The peak spacing is very reproducible for the junctions made under analogous processing conditions. While remaining always in a few tens of mV, the spacing varies uncontrollably either for different batches of the same solutions or for different substrate material. For T3 spacings from 22 to 50 mV have been

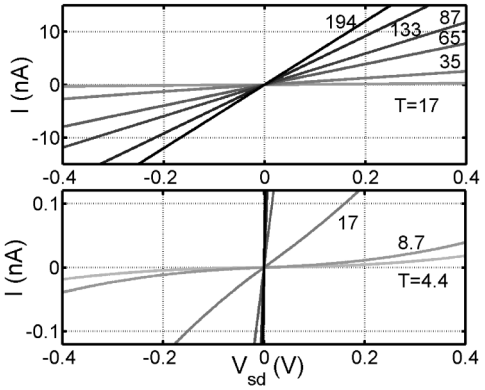

FIG. 2. Typical *I-V* characteristics of a Au-T3-Au junction for a single grain sample at different temperatures.

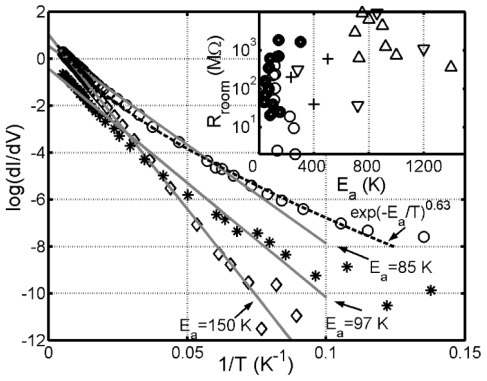

FIG. 3. Examples of temperature dependence of conductance for different Au-T3-Au single grain samples. The lines are fits with Ahrrenius low. The best fits are achieved with modified exponential law with $0.6 < \alpha < 0.9$ for different samples ($\alpha = 0.63$ shown). Inset: Activation energies observed for different samples: ● Au-T3-Au single grain samples; ○ Au-T3-Au multigrain samples (see below); + Pd-T3-Pd junctions; △ Au-T3-Pd junctions; ▽ Pd-T3-Au junctions.

observed. The position of the peaks is affected by gate voltage. The gating can be achieved either by a buried gate fabricated on one of the rod faces [20] or by a remote metal plate.

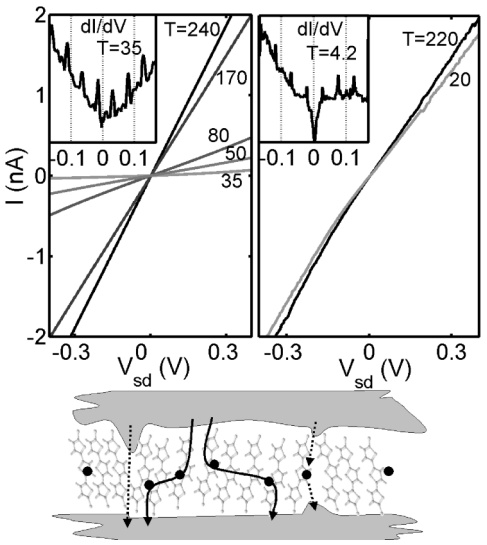

FIG. 4. Typical *IV* characteristics measured for Au-T3-Au multigrain junctions. The temperature dependent part of the conductance can be larger (left) or smaller (right) than the tunneling conductance remaining at low temperature. Insets: Differential conductance at low temperature obtained by numerical differentiation of *IV* characteristics. The peaks are the Coulomb blockade related features. Bottom: The minimal model that incorporates all essential experimental finding. The molecules do not form good bonds to both metal electrodes simultaneously. Electron transport through well-packed monolayer is dominated by the hopping through low-energy states. Tunneling likely occurs at the grain boundaries near packing defects. The sequential tunneling through an intermediate low-energy state can display the Coulomb staircase.

The observed dominant conductance mechanisms strongly suggest that generally no molecule inside the junctions, despite having reactive thiol terminations, is bonded to both metal electrodes. According to most calculations, tunneling conductance of the order of $\sim 10^{-6}$–$10^{-8}\ \Omega^{-1}$ can be expected for a single conjugated molecule [10,13]. While these values are in the range of experimentally measured junction conductance at room temperature, the conductance is thermally activated and it vanishes at zero temperature. The naive picture that the top electrode is supported by the monolayer conformly sticking to the molecules is not valid. Instead, the metal forms a grainy surface effectively delaminating from the monolayer or lifting the molecules from the bottom electrode.

Another unexpected result is the consistent observation of the small activation energy for all junctions. The anticipated energy scale for thermally activated transport through molecules is in the range of eV but not meV. The variation of E_a with metal type clearly shows that interactions between the metal electrodes and the molecules are important. The exact lineup between the molecular levels and the Fermi level sensitively depends on the strength of the sulfur-metal bond, the hybridization between metal and molecular states and the formation of interfacial dipole. One possibility is that the attachment sites and bond strength vary strongly within the monolayer creating hybridized states at all energies. Some of these states fall close in energy to the Fermi level.

An alternative possibility is that the low-energy states tied to the Fermi level originate from metal atoms mixed with molecular states. Noble metals are known to form only weak bonds with organic compounds [23–25] possibly creating states close to the Fermi level. While metal atoms can penetrate into the SAM during the evaporation of the top contact [19], our results demonstrate that the energy scale is determined by the combined nature of both contacts. The evidence for low-energy states is seen in other experiments that do not employ metal evaporation for the second electrode [9–11]. Possibly, the metal diffusion happens also during the self-assembly process concurrently with metal surface modification [16].

Other important feature is the strong temperature dependence of conductance at source-drain bias V_{sd} much larger than the scale of the activation energy. In the case of usual sequential tunneling, conductance is suppressed at energies smaller than the energy gap only. At larger biases, tunneling electrons gain energy from the applied electric field and the conductance is determined by the fixed tunnel barriers [26]. In the present case, electrons must hop perpendicular to the electric field while crossing the SAM from the source to the drain (Fig. 4). The in-layer hopping is the rate-limiting step for the low-temperature transport.

Formation of metal filaments partly or fully penetrating through the SAM can strongly affect the apparent conductance mechanism. Present results show that the

filament formation sensitively depends on the morphology of the SAM substrate. Of all samples, only the smallest junctions made on Sh1 tips display no tunneling conductance. We suggest that these junctions are formed on a single-grain of the drain electrode. The SAM is well packed suppressing metal penetration during the evaporation [18,27]. The top electrode can be partly supported by the source lead. The main difference of the Sh2 junctions is the length of the tip edge that is clearly larger than the grain size. The yield of nonshorted junctions is much lower and tunneling conductance is observed. The metal filaments are likely formed near defects in the SAM packing at the grain boundaries [15]. The junctions made on Sh3 and Sh4 tips are also multigrain junctions with a comparable number of grains. However, the yield of nonshorted junctions is noticeably higher than that on Sh2 tips. The continuous metal film growing on top of the SAM does not conform to the topography of the bottom electrode. This can result in larger average distance between the source and the drain for the rougher substrate topography, thus reducing probability of the shorting.

The periodic conductance structure [20] seen in multigrain junctions (insets to Fig. 4) is reminiscent of the Coulomb-blockade behavior. The V_{sd} period typically is a few tens of meV ruling out the possibility of the charging effects of a single molecule. The observed charging energy is typical for objects with size ~5–10 nm depending on the proximity of metal electrodes. We suggest that some low-energy states in the SAM can be multiply charged. Such a state can be delocalized over a distance of order ~5 nm within the monolayer plane [28]. Alternatively, a metal cluster split off from the top electrode can reside in the proximity of the current path. In both cases, additional assumptions are needed to account for good reproducibility of the charging energy for specific molecule types. Generally, this conductance channel is a smaller part of overall tunneling conductance.

In summary, we have determined the common conductance mechanisms for small metal-SAM-metal junctions. In all cases, the dominant room temperature conductance is hopping with small activation energies. The relative contribution of tunneling conductance strongly depends on the surface topography of the metal electrodes. In the case of metal contact evaporated on top of the SAM studied here, the mutual roughness of the metal topography is comparable with the molecular length scale. As a result, direct tunneling through the molecules is negligible. Based on a similarity with published transport data, we believe that similar issues are relevant for other methods of contacting molecules.

We gratefully acknowledge useful discussions with R. De Piccioto, E. Chandross, D. Hamman, E. Garfunkel, W. Jiang, and K. Matveev. A. E. thanks A. v. Humboldt Foundation for the financial support.

[1] J. Chen, M. A. Reed, A. M. Rawlett, and J. M. Tour, Science **286**, 1550 (1999).
[2] J. Park *et al.*, Nature (London) **417**, 722 (2002).
[3] W. Liang, M. P. Shores, M. Bockrath, J. R. Long, and H. Park, Nature (London) **417**, 725 (2002).
[4] X. D. Cui, A. Primak, X. Zarate, J. Tomfohr, O. F. Sankey, A. L. Moore, D. Gust, G. Harris, and S. M. Lindsay, Science **294**, 571 (2001).
[5] C. P. Collier, G. Mattersteig, E. W. Wong, Y. Luo, K. Beverly, J. Sampaio, F. M. Raymo, J. F. Stoddart, and J. R. Heath, Science **289**, 1172 (2000).
[6] C. Zhou, M. R. Deshpande, M. A. Reed, L. Jones, and J. M. Tour, Appl. Phys. Lett. **71**, 611 (1997).
[7] W. Wang, T. Lee, and M. A. Reed, Phys. Rev. B **68**, 035416 (2003).
[8] K.-A. Son, H. I. Kim, and J. E. Houston, Phys. Rev. Lett. **86**, 5357 (2001).
[9] Y. Selzer, M. A. Cabassi, T. S. Mayer, Y. Yao, J. M. Tour, and D. L. Allara (to be published).
[10] C. Kergueris, J. P. Bourgouin, S. Palacin, D. Esteve, C. Urbina, M. Magoga, and C. Joachim, Phys. Rev. B **59**, 12 505 (1999).
[11] S. Kubatkin, A. Danilov, M. Hjort, J. Cornil, J.-L. Bredas, N. Stuhr-Hansen, P. Hedegard, and T. Bjornholm, Nature (London) **425**, 698 (2003).
[12] M. Di Ventra, S. T. Pantelides, and N. D. Lang, Phys. Rev. Lett. **84**, 979 (2000).
[13] J. Heurich, J. C. Cuevas, W. Wenzel, and G. Schon, Phys. Rev. Lett. **88**, 256803 (2002).
[14] S. Hong, R. Reifenberger, W. Tian, S. Datta, J. Henderson, and C. P. Kubiak, Superlattices Microstruct. **28**, 289 (2000).
[15] L. A. Bumm, J. J. Arnold, M. T. Cygan, T. D. Dunbar, T. P. Burgin, L. Jones, D. L. Allara, J. M. Tour, and P. S. Weiss, Science **271**, 1705 (1996).
[16] C. Schonenberger, J. A. M. Sondaghuethorst, J. Jorritsma, and L. G. J. Fokkink, Langmuir **10**, 611 (1994).
[17] B. C. Haynie, A. V. Walker, T. B. Tighe, D. L. Allara, and N. Winograd, Appl. Surf. Sci. **203**, 433 (2003).
[18] B. d. Boer, M. M. Frank, Y. J. Chabal, W. Jiang, E. Garfunkel, and Z. Bao, Langmuir (to be published).
[19] G. Philipp, C. Müller-Schwanneke, M. Burghard, S. Roth, and K. v. Klitzing, J. Appl. Phys. **85**, 3374 (1999).
[20] N. B. Zhitenev, H. Meng, and Z. Bao, Phys. Rev. Lett. **88**, 226801 (2002).
[21] N. B. Zhitenev, A. Erbe, H. Meng, and Z. Bao, Nanotechnology **14**, 254 (2003).
[22] B. d. Boer, H. Meng, D. F. Perepichka, J. Zheng, M. M. Frank, Y. J. Chabal, and Z. N. Bao, Langmuir **19**, 4272 (2003).
[23] F. Elfeninat, C. Fredriksson, E. Sacher, and A. Selmani, J. Chem. Phys. **102**, 6153 (1995).
[24] J. Noh, E. Ito, K. Nakajima, J. Kim, H. Lee, and M. Hara, J. Phys. Chem. B **106**, 7139 (2002).
[25] A. Bratkovsky (private communication).
[26] H. Grabert and M. H. Devoret, *Single Charge Tunneling* (Plenum Press, New York, 1992).
[27] T. Ohgi, H.-Y. Sheng, Z.-C. Dong, H. Nejoh, and D. Fujita, Appl. Phys. Lett. **79**, 2453 (2001).
[28] T. Ishida, W. Mizutani, U. Akiba, K. Umemura, A. Inoue, N. Choi, M. Fujihira, and H. Tokumoto, J. Phys. Chem. B **103**, 1686 (1999).